JOURNAL OF VIROLOGY, Mar. 1996, p. 1375–1383 Vol. 70, No. 3
0022-538X/96/$04.00+0

Apoptosis Is Induced by N-*myc* Expression in Hepatocytes, a Frequent Event in Hepadnavirus Oncogenesis, and Is Blocked by Insulin-Like Growth Factor II

KEIJI UEDA AND DON GANEM*

Howard Hughes Medical Institute and Departments of Microbiology and Medicine, University of California Medical Center, San Francisco, California 94143-0414

Received 23 June 1995/Accepted 21 November 1995

Induction of hepatocellular carcinoma in woodchucks by woodchuck hepatitis virus is associated with the activation of N-*myc* gene expression, usually by viral DNA integration in *cis* to the N-*myc* locus. We have examined the consequences of N-*myc* up-regulation in rodent hepatic cells in culture. Mouse αML hepatocytes infected with a retroviral vector overexpressing the woodchuck N-*myc2* gene display a higher proliferation rate than parental αML cells but are morphologically unchanged and do not form colonies in soft agar. However, they display an increased propensity to undergo apoptosis, an effect that is markedly augmented by serum deprivation. Expression of the woodchuck hepatitis virus X gene in αML cells does not alter the growth phenotype of the cells and has no effect upon N-*myc*-dependent apoptosis. However, apoptosis in N-*myc2*-expressing αML cells is strongly inhibited by insulin-like growth factor II (IGF II). IGF II gene expression is also strongly up-regulated during hepatic carcinogenesis in vivo in virally infected animals and has been speculated to be part of an autocrine growth-stimulatory pathway. Our results suggest that IGF II may play another role in the development of virus-induced hepatoma: the prevention of programmed cell death triggered by deregulated N-*myc* expression.

Persistent infection of human hosts by hepatitis B virus (HBV) produces a 100-fold increase in risk for hepatocellular carcinoma (HCC) (1). Although much is known about HBV replication and pathogenesis, the molecular mechanism(s) by which HBV infection predisposes to HCC remains poorly understood (see references 2, 11, and 24 for reviews). Hepatomas that arise in HBV-infected patients generally lack evidence of ongoing viral replication in tumor cells, despite active replication in surrounding nontumorous liver. But most tumor cells contain multiple copies of viral DNA that is integrated into the host genome, and these integrants display a clonal pattern that indicates that integration preceded (or accompanied) the clonal outgrowth of the malignant cells. Usually, the integrants are grossly rearranged, so that no single viral gene is consistently expressed in the tumor; many integrants have lost the capacity to encode any viral protein at all (19, 29). Much attention has been directed to the possibility that these integrated genomes function to activate flanking cellular genes involved in growth control, as has been well documented in retroviral oncogenesis in several species (16). But extensive studies have not succeeded in identifying common targets of these insertion events in the human genome, and many other possibilities remain for how HBV infection relates to liver carcinogenesis (2, 11, 24).

However, in one well-developed animal model of hepadnaviral oncogenesis, insertional activation of host oncogenes by viral sequences is firmly established. Woodchucks chronically infected by the woodchuck hepatitis virus (WHV), a hepadnavirus closely related to human HBV, display a striking liver cancer risk: virtually 100% of animals infected from birth will die of HCC (21). Tumors develop in midlife (between 2 and 4 years of age), and it is not infrequent to find multiple independent tumors arising in a single infected liver (10, 12, 28). Thus, the magnitude of the oncogenic stimulus in WHV infection is even greater than that which accompanies HBV infection. But in most other regards, the tumors resemble those of HBV-related human HCCs: they harbor multiple integrated copies of viral DNA with genomic rearrangements highly reminiscent of those in HBV integrants (10, 12, 20), and viral replication is extinguished in the tumor cells (43, 44). Importantly, in ca. 40% of WHV-induced HCCs, insertions of viral DNA are found within several kilobases of the N-*myc2* locus (woodchucks contain two genomic N-*myc* loci [9, 10]); N-*myc1* is a conventional three-exon gene, while the second locus, N-*myc2*, is a processed cDNA copy which retains functional expression signals). Most of the remaining tumors also harbor WHV insertions in *cis* to N-*myc2* but up to 250 kb away (8). In all cases, the N-*myc2* gene, which is transcriptionally silent in normal adult hepatocytes, is strongly overexpressed. Since the activated transcripts emanate from their normal cellular start sites, it is presumed that viral sequences supply recognition sites for cellular transcription factors that up-regulate transcription from the N-*myc2* promoter (37).

N-*myc2* activation takes place early in oncogenesis, being readily detected by in situ hybridization even in premalignant nodules (43). These premalignant nodules display many other remarkable features, including suppression of viral gene expression and, notably, up-regulation of insulin-like growth factor II (IGF II) expression (44). Careful studies by Yang et al. (43, 44) have shown that IGF II production is a regular accompaniment of hepatic oncogenesis in woodchucks, and it has been suggested that IGF II production by the tumor might be an important autocrine proliferative signal. In this report, we suggest another potential role for IGF II production by the tumor. Hepatic cells overexpressing N-*myc2* display a striking propensity to undergo apoptosis, particularly in response to certain environmental signals leading to growth arrest, and this apoptotic response is abrogated by the presence of IGF II. This finding suggests that an important role of IGF II expression by

* Corresponding author. Fax: (415) 476-0939. Electronic mail address: ganem@socrates.ucsf.edu.

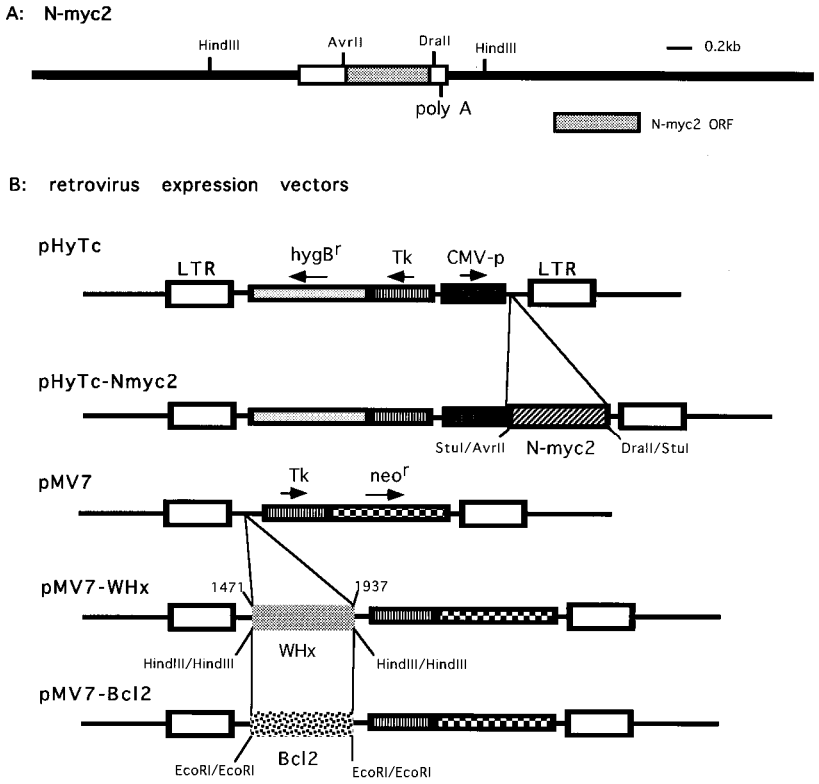

FIG. 1. (A) The WHV N-*myc2* gene. The stippled area denotes the N-*myc2* open reading frame (ORF); relevant restriction sites are shown. (B) Structures of murine leukemia virus expression vectors. pHyTc bears a hygromycin resistance allele (hygB^r) driven by the herpes simplex virus thymidine kinase (Tk) promoter, cloned in the opposite orientation to the viral long terminal repeat (LTR). A cytomegalovirus immediate-early promoter (CMV-p) is present in the same orientation as the long terminal repeat and is upstream of a polylinker into which the N-*myc2* gene has been cloned in pHyTc-Nmyc2. pMV7 carries a neomycin resistance marker (neo^r) driven by the thymidine kinase promoter; 5′ to this selectable marker is a polylinker into which have been cloned the WHV X gene (WHx; in pMV7-WHx) and the *bcl2* gene (in pMV7-Bcl2) at the indicated restriction sites.

the tumor cells may be the prevention of cell death triggered by N-*myc* deregulation.

MATERIALS AND METHODS

Plasmid constructions. The retroviral vectors used in this work are schematically depicted in Fig. 1. For the N-*myc2* recombinant, we purified an *Avr*II-*Dra*II fragment from an N-*myc2* gene cloned from normal woodchuck liver DNA and inserted it into the *Stu*I site of the pHyTc retroviral vector, which was modified from pLNC-X (18) by blunt-end ligation. In this vector, which also carries a hygromycin resistance marker, N-*myc2* expression is driven by a cytomegalovirus immediate-early promoter. All other recombinant retroviral vectors were made in the pMV7 vector, which carries a G418 resistance marker and in which expression of the inserted gene is driven by the murine leukemia virus long terminal repeat. For the WHV X-gene expression vector, the WHV X-gene coding region from nucleotides 1471 to 1937 (numbering system of Kodama et. al. [15]) was amplified by PCR and inserted into the *Hin*dIII site of pMV7. The resulting X gene was verified by DNA sequencing to be free of mutations. The pMV7-Bcl2 vector was constructed by Wagner et al. (35) and was kindly supplied by Nissim Hay (University of Chicago).

Cells, viruses, and transformations. To generate viral stocks from the vectors described above, we transfected the ecotropic packaging cell line PE501 (17) with the indicated plasmid and selected stable transformants resistant to the corresponding drug; both hygromycin B and G418 were used at 250 μg/ml. The titers of infectious virus particles in the supernatants from these transformants were determined by plating on Rat-1 cells and were typically in the range of 10^5/ml, though plating on αML cells usually revealed substantially fewer drug-resistant foci; the reasons for this have not been systematically examined.

αML cells were the kind gift of Nelson Fausto (University of Washington, Seattle) (42). To produce transductants bearing N-*myc2*, *bcl-2*, or the WHV X gene, the cells were infected with 3 ml of viral stocks and drug-resistant cells were selected. Multiple individual foci were expanded and tested for expression of the vector-expressed gene by Northern (RNA) blotting, and colonies with correctly expressed transcripts were saved for further analysis. Two well-characterized αML clones bearing N-*myc2* were used for all experiments, including the generation of WHV X-gene- and *bcl2*-expressing derivatives. In all cases the biological behaviors of these two lines and their derivatives were indistinguishable; data from only one set of clones are presented. In addition, a mass culture of N-*myc2*-expressing αML cells containing a pool of over 100 independent transductants was examined for growth properties.

Northern blotting analysis. RNA was extracted from αML cells by the hot-phenol method from semiconfluent cells in 10-cm-diameter plates (Corning), and poly(A)$^+$ RNA was selected with oligo(dT) latex beads (Daiichi). Two micrograms of this RNA was electrophoresed through 1.2% agarose–2.2 M formaldehyde gels, transferred to nylon membranes, and hybridized to ^{32}P-labeled DNA probes specific for the appropriate inserted gene as described previously (26).

Cell growth assay. Pools of ca. 100 individual hygromycin-resistant transformants were selected following infection of αML cells with viruses derived from pHyTc or pHyTc-Nmyc2. For each pool, cells were seeded at 10^5/6-cm-diameter dish (Corning); thereafter, viable cells (as determined by the trypan blue exclusion method) were counted in a hemocytometer every 24 h, and the results were expressed as the number of cells per dish. Each time point was the mean of quadruplicate measurements.

Cell viability assays. Cell viability was assessed by trypan blue exclusion. For each time point, percent cell death was determined by $Dt/Vt + Dt$, where Dt is the number of dead cells at time t and Vt is the number of viable cells at time t. As an indirect measure of viability, we also used the MTT (3-[4,5 dimethylthiazol-2-yl]-2,5-diphenyl tetrazolium bromide) assay (30). Cells were seeded at 5×10^4 per well in 24-well dishes. At the times selected for assay, the cells were washed twice with phosphate-buffered saline (PBS; GIBCO) and suspended in growth medium; after a further 2 h, a 1/10 volume of a 3-mg/ml solution of MTT in PBS was added (i.e., to a final MTT concentration of 0.3 mg/ml). Incubation was continued for another 3 h, and the resulting formazan was solubilized in MTT solubilization solution (10% Triton X-100–0.1 N HCl in anhydrous isopropanol). The A_{570} and A_{690} of this material were then determined spectrophotometrically, and the value $A_{570} - A_{690}$ was computed. All assays were performed on quadruplicate wells of cells, and the results are displayed as the means and standard deviations of these four measurements.

DNA fragmentation assay. At the indicated times postplating, cells were harvested from the dishes and medium, and total DNA was extracted from the

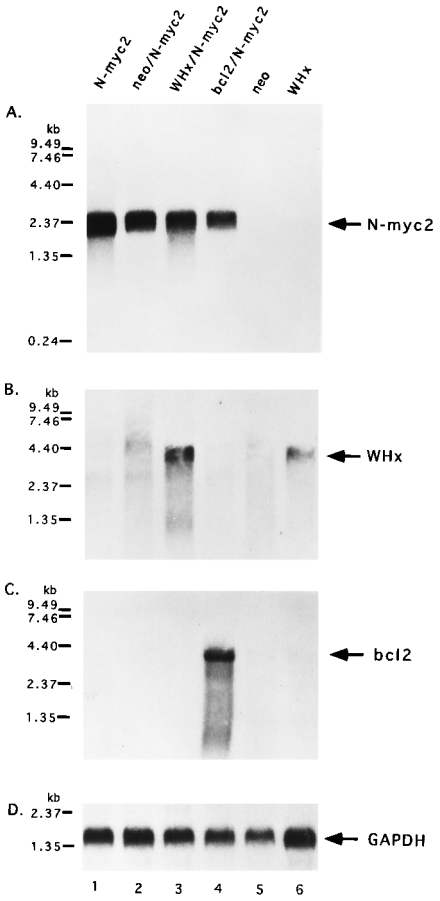

FIG. 2. Northern analysis of transcripts produced by retroviral vectors. Poly(A)$^+$ RNA was prepared from clonal αML cell lines infected with the following viral vectors: pHyTc-Nmyc2 (lane 1); pMV7 plus pHyTc-Nmyc2 (lane 2); pMV7-WHx plus pHyTc-Nmyc2 (lane 3); pMV7-Bcl2 plus pHyTc-Nmyc2 (lane 4); pMV7 (lane 5); and pMV7-WHx (lane 6). RNA was electrophoresed in agarose-formaldehyde gels, transferred to solid supports, and annealed to ^{32}P-labeled DNA probes homologous to N-*myc2* (A), WHV X (B), *bcl2* (C), or *GAPDH* (D).

pooled cells by lysis with 0.5% sodium dodecyl sulfate and proteinase K (500 μg/ml) followed by phenol extraction and ethanol precipitation. Ten micrograms of this DNA was electrophoresed through 1.5% agarose gels containing 5 μg of ethidium bromide per ml and examined on a UV transilluminator.

DAPI staining. Cells were examined before or 6 h after serum deprivation. The cells were fixed with 3.7% formaldehyde–0.01% Triton X-100 in PBS for 30 min, stained with 50 μg of DAPI (4,6-diamidino-2-phenylindole) per ml for 10 min, and then examined microscopically under UV illumination as previously described (15a).

RESULTS

N-*myc2* expression in mouse hepatocytes. To better understand the phenotypic consequences of N-*myc* deregulation, we sought to introduce activated N-*myc* alleles into cultured cells of hepatic origin. The activated allele that we constructed is shown in Fig. 1; it contains a wild-type N-*myc2* coding region under the control of a cytomegalovirus immediate-early promoter/enhancer in a retrovirus (murine leukemia virus) vector that also bears a hygromycin resistance gene. This plasmid construct (together with a *lacZ*-expressing plasmid) was transfected by lipofection into primary rat hepatocytes, which are highly differentiated, nondividing cells with a limited (3-week) life span in culture. Although expression of *lacZ* was readily detectable in the recipient cells by X-Gal (5-bromo-4-chloro-3-indolyl-β-D-galactopyranoside) staining, no immortal or transformed foci emerged in the presence or absence of hygromycin selection. (By contrast, when 1 μg of a plasmid expressing simian virus 40 T antigen was similarly transfected into the same cells, 20 to 40 colonies per 10^6 cells were reproducibly observed, confirming that the failure to observe such immortalized colonies by N-*myc2* transfection was not the result of the failure to achieve stable nuclear delivery of DNA.) We also generated a retroviral stock based on the pHyTc-Nmyc2 construct by transfecting it into the ecotropic packaging cell line PE501 (see Materials and Methods). The resulting viral stock had a titer of over 10^6 hygromycin-resistant CFU/ml on 3T3 or Rat-1 fibroblasts, but again no stable hygromycin-resistant transformants were observed when the stock was plated on rat primary hepatocytes. (This result may also relate to the known inefficiency with which most retroviral vectors establish proviruses in nondividing cells [25, 33].)

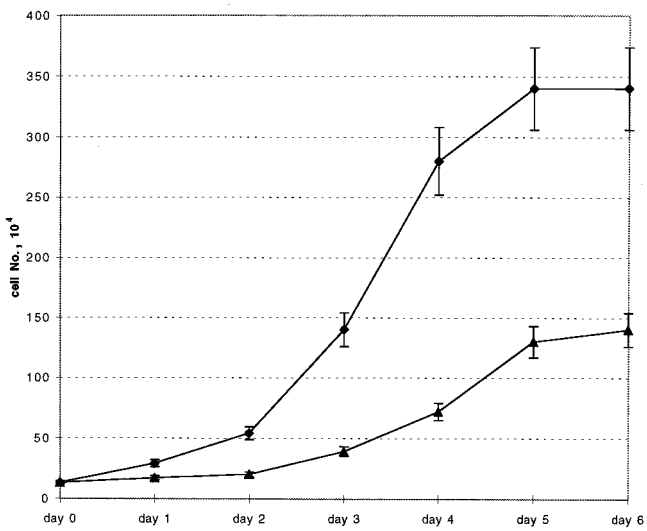

FIG. 3. Growth properties of αML cells expressing N-*myc2*. Pools of >100 hygromycin-resistant transformants derived by infection with either pHyTc (triangles) or pHyTc-Nmyc2 (diamonds) were cultured under identical conditions in parallel. At each indicated time point, viable cells were counted in a hemocytometer; each value shown is the mean of quadruplicate measurements.

Because of the difficulties associated with working with primary hepatocytes, we opted to work with a well-differentiated rodent hepatocyte line that was already immortalized but nontumorigenic. The best-characterized such line is αML, a mouse hepatocyte line derived from the liver of a transgenic mouse constitutively expressing transforming growth factor alpha under the control of the mouse metallothionein promoter (14, 42). The line is immortal but very well differentiated. It expresses a battery of liver-specific markers (including albumin, transferrin, and alpha-1 antitrypsin); interestingly, when exposed to serum-free medium, it stops dividing and undergoes further hepatocellular differentiation (42). It is permissive for the transcription and replication of both HBV and WHV, which is itself a stringent marker of hepatocytic differentiation (32a). Most importantly, it is morphologically normal, fails to grow in soft agar, and is nontumorigenic in nude mice (42). αML cells were infected with the N-*myc2*-bearing retroviral stock, and numerous hygromycin-resistant foci [designated αML(N-myc2)] were identified, cloned, and expanded. In addition, more than 100 hygromycin-resistant transductants from one plate were pooled into a mass culture that was also carried forward for analysis. Control cell lines [designated αML(hy-

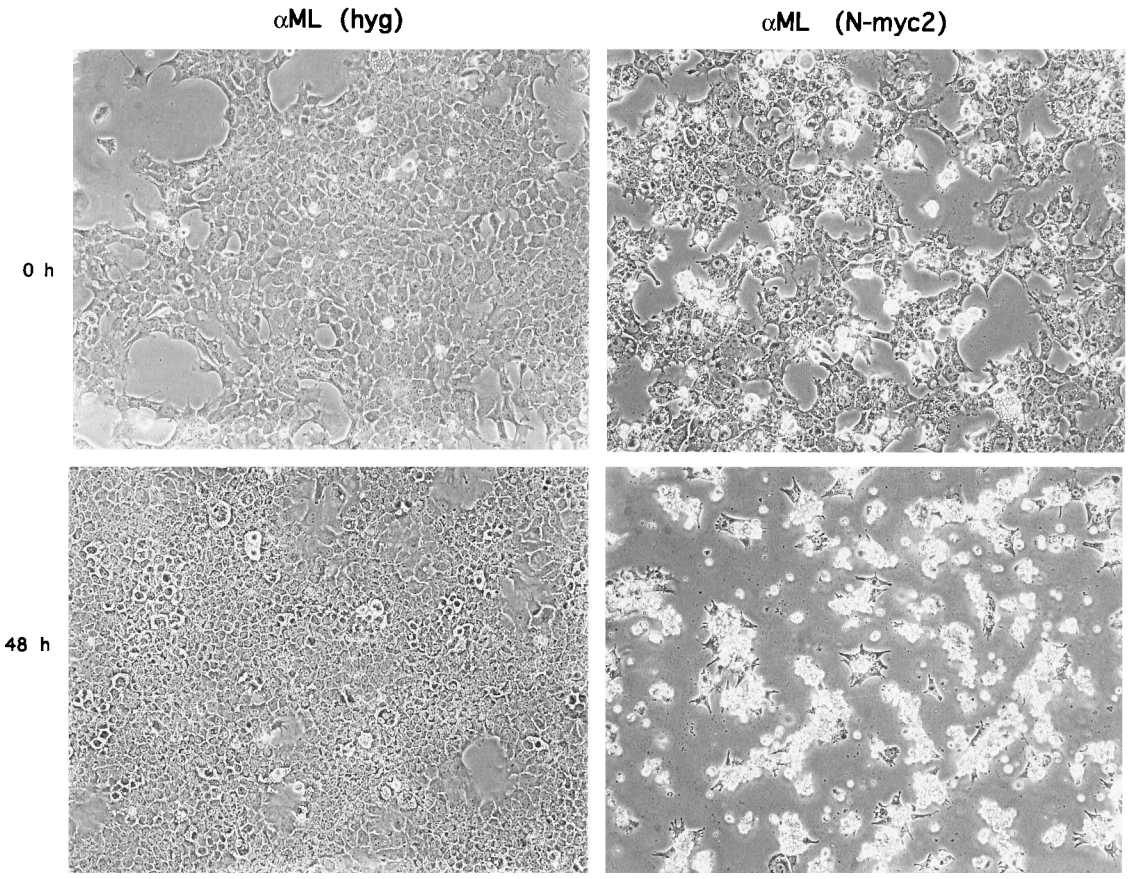

FIG. 4. Cell death induced by N-*myc2* expression and serum deprivation. αML(hygro) and αML(N-myc2) cells were plated in 0.05% serum, and samples were photographed at 0 and 48 h after serum deprivation.

gro)] were also generated by infection with the parental retroviral vector. The mass culture and most of the αML(N-myc2) clones expressed N-*myc2* RNA transcripts of the appropriate size; representative examples are shown in Fig. 2A. The αML (N-myc2) cells displayed a normal morphology and were indistinguishable microscopically from hygromycin-resistant transformants derived by infection with the parental retroviral vector lacking N-*myc2*. The αML(N-myc2) cells did, however,

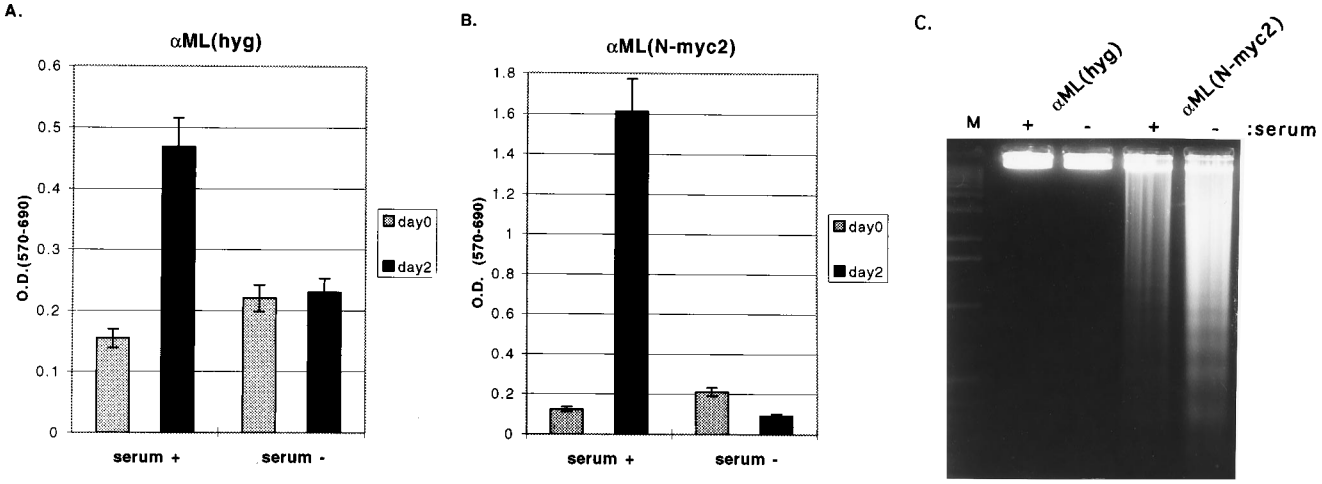

FIG. 5. Cell death and DNA fragmentation in αML(N-myc2) cells before and after serum deprivation. (A) MTT assay of αML(hygro) cells with (+) and without (−) serum on days 0 and day 2. (B) MTT assay of aML(N-myc2) cells with and without serum on days 0 and 2. (C) DNA fragmentation assay. Total cell DNA from the indicated cell lines was prepared as described in Materials and Methods and examined by agarose gel electrophoresis and ethidium bromide staining. M, molecular size standards. O.D.(570-690), optical density at 570 nm minus optical density at 690 nm.

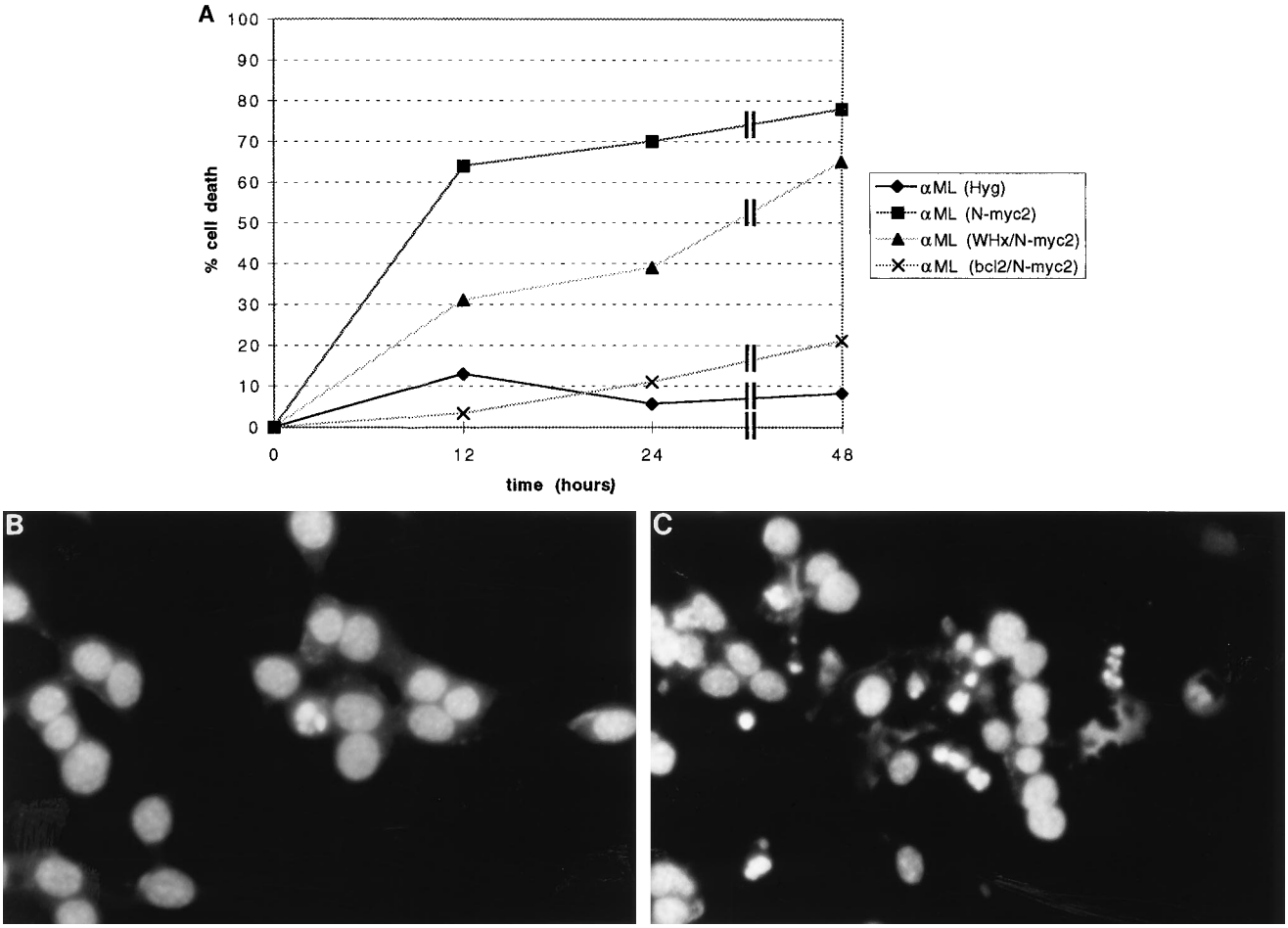

FIG. 6. Cell viability and nuclear morphology of αML cell derivatives after serum deprivation. (A) The indicated αML cell transductants were transferred to serum-free medium, and the percentage of inviable cells, as determined by the inability to exclude trypan blue, was determined at each indicated time point as described in Materials and Methods. (B) DAPI staining of αML(N-myc2) cells in the presence of serum. Note rare cell with nuclear changes characteristic of apoptosis. (C) DAPI staining of αML(N-myc2) cells 6 h after serum deprivation, showing extensive evidence of nuclear fragmentation and condensation typical of apoptosis.

display a clearly shorter doubling time and reproducibly grew to a higher saturation density (Fig. 3) than the αML or αML-(hygro) cells. In addition, the N-*myc2* transformants displayed increased mitochondrial metabolic activity, as judged by MTT metabolism (see below). However, both the mass culture of αML(N-myc2) transformants as well as the two well-characterized αML(N-myc2) clones failed to grow in soft agar.

Apoptosis in αML(N-myc2) cells. Fibroblasts overexpressing c-*myc* are known to undergo apoptosis at increased rates, and this cell death is remarkably stimulated by serum deprivation and other growth-arresting signals (7). We wondered if the same would be true of hepatocytes expressing N-*myc2*, especially since mature hepatocytes are normally growth arrested. Accordingly, we examined the growth of αML(N-myc2) cells in the presence or absence of serum. αML(hygro) or αML(N-myc2) cells were seeded into six-well plates in duplicate at 10^5 cells per dish; after 24 h in 10% serum-containing medium, the serum concentration in the medium of one half of the dishes was changed to 0.05%, and observation continued for another 48 h. Growth ceased in the serum-deprived αML(hygro) cells and a few cells detached from the plate, but the dish remained confluent with viable cells. By contrast, in αML(N-myc2) cells, massive cell death was evident by 48 h following serum deprivation (Fig. 4). To obtain a semiquantitative estimate of the extent of this cell death, we used the MTT assay (30). In this assay, cells are exposed to the compound MTT; surviving cells take up the compound and convert it to formazan, which is detected spectrophotometrically (see Materials and Methods). As shown in Fig. 5, αML(hygro) cells remain viable after 48 h, but for the αML(N-myc2) cells there is a sharp decline in the ability to metabolize MTT by 48 h after serum deprivation.

TABLE 1. Apoptosis following serum deprivation of αML cell lines[a]

Sample	No. of cells counted	Cell death (%)
αML(hygro)	162	<1
αML(N-myc2)	297	39
αML(bcl2/N-myc2)	328	5.8
αML(N-myc2) + IGF I	416	4.6
αML(N-myc2) + IGF II	294	6.1

[a] The indicated cell lines were serum deprived and examined 6 h later by DAPI staining as described in Materials and Methods. For each line, the indicated number of cells was scored for the characteristic apoptotic changes of nuclear condensation and fragmentation (see Fig. 6C), and results are expressed as the percentage of total cells scored that showed such changes.

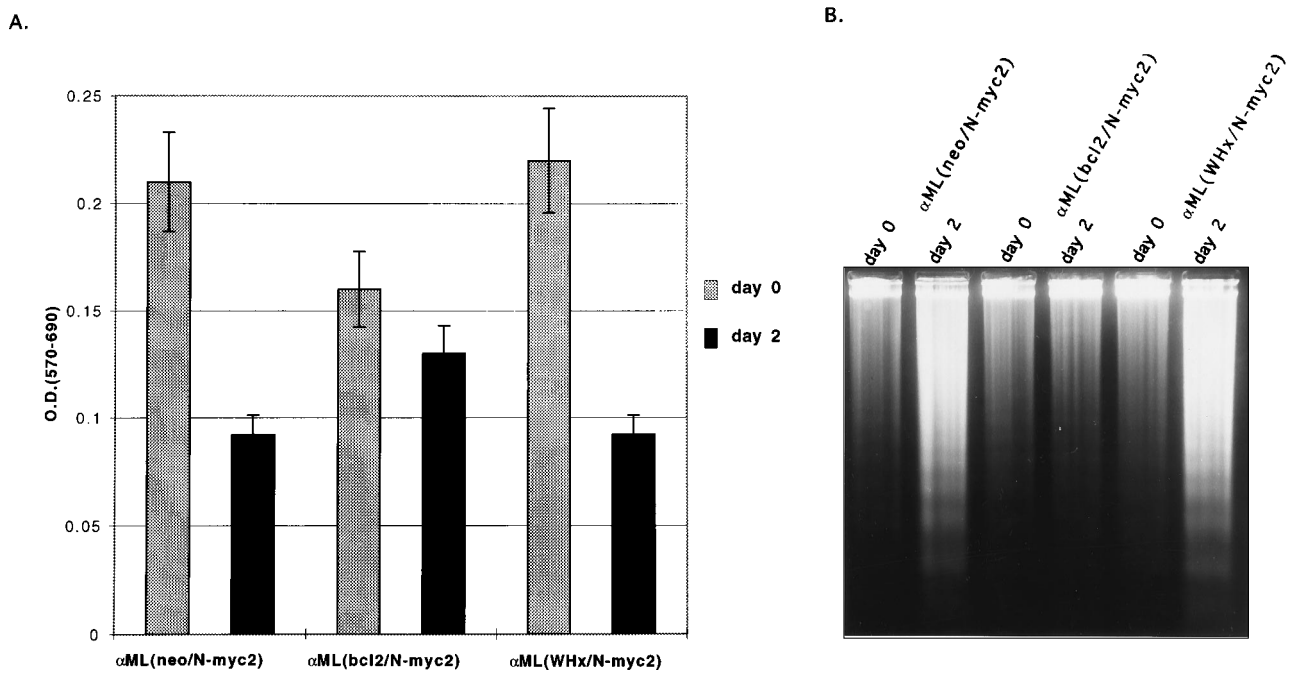

FIG. 7. *bcl2* but not WHV X-gene expression blocks N-*myc2*-induced apoptosis in response to serum deprivation. (A) MTT assay values on day 0 and on day 2 after serum deprivation. (B) DNA fragmentation pattern from N-*myc2*-expressing cultures following serum starvation. DNA was prepared from the indicated cell lines at 0 and 48 h, electrophoresed through 1.25% agarose, and stained with ethidium bromide. O.D.(570-690), optical density at 590 nm minus optical density at 690 nm.

We then examined whether this cell death was accompanied by fragmentation of the chromosomal DNA in a nucleosomal pattern, an event characteristic of the apoptotic death pathway. High-molecular-weight DNA was extracted from αML(hygro) and αML(N-myc2) cells after 48 h in the presence or absence of serum and analyzed by agarose gel electrophoresis. No degradation of the cell DNA was observed in αML(hygro) cells cultured with or without serum (Fig. 5C). By contrast, genomic fragmentation is marked in the αML(N-myc2) cells following serum deprivation (Fig. 5C). Close inspection also reveals that there is a detectable, though modest, increase in DNA degradation in the αML(N-myc2) cells even in the presence of serum. This result is consistent with earlier studies of c-*myc*-expressing fibroblasts, in which a somewhat enhanced level of apoptosis was observed even in growing cultures in the presence of serum (7); this cell loss is compensated for by the increased proliferation driven by *myc* expression under these conditions.

Since the MTT assay actually measures mitochondrial function and only indirectly indicates cell viability, we also conducted independent and more direct assays of cell death. First, viable αML(N-myc2) cells were quantitated by the ability to exclude trypan blue following serum deprivation. As shown in Fig. 6A, serum starvation led to a rapid and profound increase in cell death in αML(N-myc2) cells compared with αML(hygro) cells. When the nuclear morphology of the cells was examined by DAPI staining, a dramatic increase in nuclear fragmentation and condensation was observed as early as 6 h after serum deprivation (Fig. 6B and C); these nuclear changes are characteristic of apoptosis. We estimate (Table 1) that nearly 40% of the αML(N-myc2) cells were apoptotic by 6 h after serum withdrawal, compared with ca. 5% in the presence of serum; by contrast, apoptotic cells were not detected in αML (hygro) cultures even after serum starvation (Table 1). The finding of low but detectable apoptosis of αML(N-myc2) cells in the presence of serum accords well with the enhanced DNA fragmentation observed under these conditions (Fig. 5C).

N-*myc2*-induced cell death is blocked by *bcl-2* but not by WHV X-gene expression. If N-*myc2* up-regulation induces an apoptotic signal in hepatocytes, then some means of counteracting or negating this signal must be required during oncogenesis. Since some oncogenic viruses produce proteins that act to block cell death induced by a variety of stimuli (22, 38–41), we wondered if WHV might encode such a factor. The leading candidate viral gene for such a role would be the viral X gene, whose product is a poorly understood regulatory molecule that is dispensable for replication in cell culture but essential for growth in vivo (4, 45). Accordingly, we constructed a retroviral vector expressing the WHV X-gene coding region; as a control, we used a similar vector expressing the cellular gene *bcl2*, whose protein product is known to block apoptosis induced by a wide variety of stimuli (6, 22, 23). These vectors (Fig. 1) employ neomycin resistance as the selectable marker, facilitating isolation of the corresponding derivatives of the hygromycin-resistant αML(N-myc2) cells. We generated derivatives bearing either the pMV7neo vector alone [αML-(neo/N-myc2)], the *bcl2* vector [αML(bcl2/N-myc2)], or the WHV X-gene vector [αML(WHx/N-myc2)]. Northern blot hybridization analysis confirmed the expression of *bcl2* and WHV X-gene transcripts of the expected sizes in the corresponding transductants (Fig. 2).

These cell lines were then tested for cell death (by trypan blue exclusion) and DNA fragmentation before and after 48 h of serum deprivation; representative results are presented in Fig. 6A and 7. As can be seen, cell death (Fig. 6A) and DNA degradation (Fig. 7) were strongly inhibited by *bcl2* expression. When nuclear morphologic changes characteristic of apoptosis were scored by DAPI staining, *bcl2* expression was likewise found to strongly reduce N-*myc2*-dependent apoptosis (Table 1). Although transduction by the WHV X-gene expression

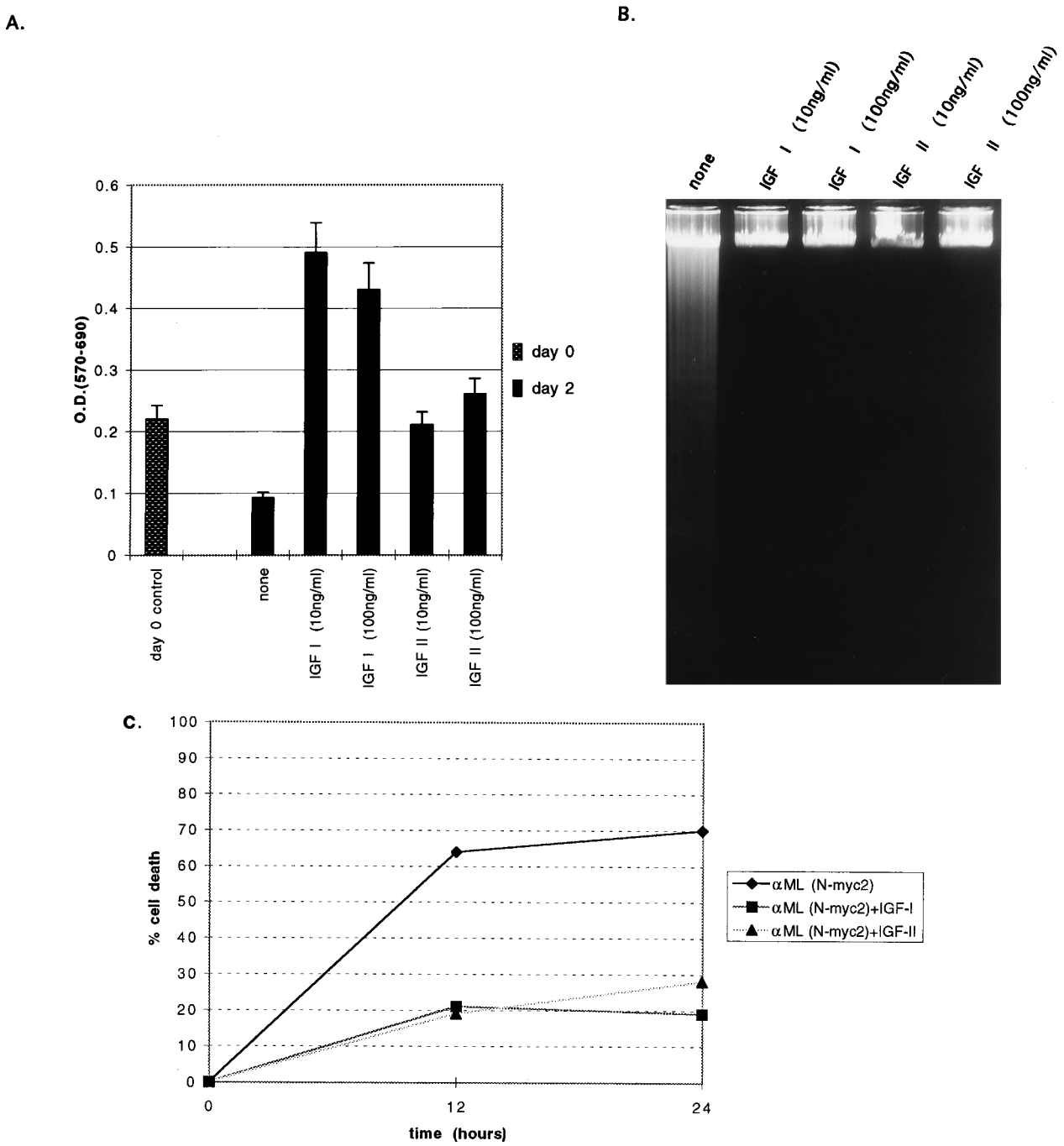

FIG. 8. IGF I and II block apoptosis triggered by serum deprivation in αML(N-myc2) cells. (A) MTT assay. αML(N-myc2) cells were grown to semiconfluence, and then medium was replaced with medium containing 0.05% serum and the indicated concentrations of IGF I or IGF II; after 48 h of further incubation, the MTT assay was performed. MTT assay values at time zero of serum deprivation and after 48 h of serum deprivation in the presence of the indicated growth factor are shown. O.D.(590-690), optical density at 590 nm minus optical density at 690 nm. (B) DNA fragmentation assay. DNA from αML(N-myc2) cells was prepared after 48 h of serum deprivation in the presence of the indicated concentrations of IGF I or IGF II; DNA was electrophoresed in agarose gels and stained with ethidium bromide. (C) Cell inviability assay. αML(N-myc2) cells were transferred to serum-free medium in the absence or presence of IGF-I or IGF-II, and the percentage of dead cells was determined by trypan blue staining at each indicated time point. The 12-h time point precedes the onset of any increase in cell number in the IGF-I-treated culture.

vector detectably slowed the kinetics of cell death (Fig. 6A), it did not greatly reduce its final extent, nor did it prevent the DNA fragmentation characteristic of apoptosis (Fig. 7). In fact, X-gene expression in αML cells (with or without N-*myc2* expression) conferred no detectable phenotype with regard to morphology, serum dependence, or growth in soft agar (data not shown).

Inhibition of hepatocellular apoptosis by IGF II. In the absence of a known viral inhibitor of apoptosis, it seemed likely that a cellular gene product might serve this function during hepatic carcinogenesis. In reviewing the literature on gene expression in HCC, we were struck by the frequent occurrence of the expression of IGFs in hepatoma cells of many species (3, 31, 43, 44). In WHV-mediated liver oncogenesis, for example,

the vast majority of overt HCCs express IGF II mRNA and protein (43, 44). In fact, as noted earlier, IGF II mRNA is expressed in the earliest known precancerous hepatic lesions, in parallel with N-*myc2* RNA (43). We were especially interested in IGFs because of their known ability to blunt programmed cell death in fibroblastic cells overexpressing c-*myc* (13). Accordingly, we examined the ability of IGF I and IGF II to block the apoptotic response of αML(N-myc2) cells to serum deprivation. As shown in Fig. 8C, both IGF I and IGF II prevented the rapid and early death of N-*myc2*-expressing hepatocytes, as judged by trypan blue exclusion; they also efficiently blocked DNA degradation under these conditions (Fig. 8B). Consistent with this finding, both proteins led to a dramatic reduction in morphologically apoptotic cells within 6 h of serum deprivation, as revealed by DAPI staining (Table 1). IGF I also appears to possess powerful growth-stimulatory properties for αML(N-myc2) hepatocytes, leading to an increase in cell number by 48 h (not shown) and a corresponding increase in MTT conversion (Fig. 8A) even at concentrations as low as 10 ng/ml. By contrast, IGF II, which efficiently blocked cell death, had only a small effect on cell number (not shown) and MTT conversion (Fig. 8A), even at high concentrations.

DISCUSSION

These results demonstrate that activation of N-*myc2* expression in hepatic cells does not greatly affect their morphology or fully transform them but does enhance their proliferation and generates a marked predisposition to apoptosis under certain environmental conditions. The modest effect of N-*myc2* on cell growth is consistent with what is known about WHV-induced oncogenesis in vivo. Cells expressing N-*myc2* are found early in the oncogenic sequence, months to years before the development of overt carcinoma, and cells in these early preneoplastic foci have few morphologic changes. Presumably this is only one of many genetic lesions required for the full expression of the malignant phenotype, setting the stage for subsequent mutations by conferring an incremental growth advantage over surrounding cells and resulting in more cells undergoing DNA replication. However, the tendency toward apoptosis would be expected to impede this progression, leading to a selection for cells that can blunt the apoptotic response. We propose that the up-regulation of IGF II regularly observed during oncogenesis arises in response to this selection and serves principally to effect such inhibition. A similar role has been posited for IGF expression during the progression of experimental insulinomas in transgenic mice expressing simian virus 40 T antigen in pancreatic islet cells (5). We cannot exclude an additional role for IGF II as a proliferative stimulus, but such effects were modest in our cell culture system; IGF-I, by contrast, had quite dramatic growth-promoting activity in this system, in addition to its antiapoptotic effects.

It has been well established recently that many oncogenic viruses generate products that influence the apoptotic responses of the host. For example, adenovirus E1A protein activates p53 expression during infection; this would lead to induction of apoptosis (22, 38, 39) were it not for products of the E1B locus that prevent this response. In this way, premature cell suicide is prevented, allowing the virus to complete its replication cycle. E1B products are also important for cell transformation mediated by adenovirus. Recently, it has been shown that *myc*-induced apoptosis involves the p53 pathway (34). In view of recent suggestions that the hepadnavirus X protein can bind p53 in vitro (32, 36), we were particularly interested in the possibility that the viral X protein might be involved in the prevention of apoptosis during N-*myc*-induced oncogenesis. However, we were unable to firmly demonstrate such a role for WHV X protein in our experimental system, and the true in vivo function of this protein remains unclear.

Although our experiments were conducted on immortalized hepatocytes in culture, we think it likely that the results are relevant to hepatocytes in vivo. We note with interest that attempts to generate transgenic mice overexpressing N-*myc2* in the liver have met with great difficulties (7a). Although the reasons for this are unknown, the phenotype suggests that hepatic overexpression of N-*myc* is not tolerated in vivo and is consistent with the possibility that apoptosis is induced by N-*myc* in vivo.

REFERENCES

1. **Beasley, R. P.** 1988. Hepatitis B virus-the major etiology of hepatocellular carcinoma. Cancer **61:**1942–1956.
2. **Buendia, M. A.** 1992. Hepatitis B viruses and hepatocellular carcinoma. Adv. Cancer Res. **59:**167–226.
3. **Cariani, E., C. Lasserre, and D. Seurin.** 1988. Differential expression of IGF-II mRNA in human primary liver cancers, benign liver tumors and liver cirrhosis. Cancer Res. **48:**6844–6849.
4. **Chen, H.-S., S. Kaneko, R. Girones, R. W. Anderson, W. E. Hornbuckle, B. C. Tennant, P. J. Cote, J. L. Gerin, R. H. Purcell, and R. H. Miller.** 1993. The woodchuck hepatitis X gene is important for establishment of virus infection in woodchucks. J. Virol. **67:**1218–1226.
5. **Christofori, G., P. Naik, and D. Hanahan.** 1994. A second signal supplied by insulin-like growth factor II in oncogene-induced tumorigenesis. Nature (London) **369:**414–418.
6. **Ellis, R. E., Y. Yuan, and H. R. Horvitz.** 1991. Mechanisms and functions of cell death. Annu. Rev. Cell Biol. **7:**663–698.
7. **Evan, G., A. Wyllie, C. Gilbert, T. Little wood, H. Land, M. Brooks, C. Waters, L. Penn, and D. Hancock.** 1992. Induction of apoptosis in fibroblasts by c-myc protein. Cell **69:**119–128.

7a. **Fourel, G., and M.-A. Buendia.** Personal communication.

8. **Fourel, G., J. Couturier, Y. Wei, F. Apiou, P. Tiollais, and M.-A. Buendia.** 1994. Evidence for long-range oncogene activation by hepadnavirus insertion. EMBO J. **13:**2526–2534.
9. **Fourel, G., C. Transy, B. C. Tennant, and M.-A. Buendia.** 1992. Expression of the woodchuck N-*myc2* retroposon in brain and liver tumors is driven by a cryptic N-*myc* promoter. Mol. Cell. Biol. **12:**5336–5344.
10. **Fourel, G., C. Trepo, L. Bougueleret, B. Henglein, A. Ponzetto, P. Tiollais, and A.-A. Buendia.** 1990. Frequent activation of N-myc genes by hepadnavirus insertion in woodchuck liver tumours. Nature (London) **347:**294–298.
11. **Ganem, D., and H. E. Varmus.** 1987. The molecular biology of the hepatitis B viruses. Annu. Rev. Biochem. **56:**651–693.
12. **Hansen, L. J., B. C. Tennant, C. Seeger, and D. Ganem.** 1993. Differential activation of *myc* gene family members in hepatic carcinogenesis by closely related hepatitis B virus. Mol. Cell. Biol. **13:**659–667.
13. **Harrington, E. A., M. R. Bennett, A. Fanindi, and G. I. Evan.** 1994. c-myc-induced apoptosis in fibroblasts is inhibited by specific cytokines. EMBO J. **13:**3288–3295.
14. **Jhappan, C., C. Stahle, R. N. Harkins, N. Fausto, G. H. Smith, and G. T. Merlino.** 1990. TGFα overexpression in transgenic mice induces liver neoplasia and abnormal development of the mammary gland and pancreas. Cell **61:**1137–1146.
15. **Kokama, K., Ogasawara, H. Yoshikawa, and S. Murakami.** 1985. Nucleotide sequence of a cloned woodchuck hepatitis virus genome: evolutional relationship between hepadnaviruses. J. Virol. **56:**978–986.

15a. **Kulkarni, G., and C. A. G. McCulloch.** 1994. Serum deprivation induces apoptotic cell death in a subset of Balb/C 3t3 fibroblasts. J. Cell Sci. **107:** 1169–1179.

16. **Lohuizen, M. V., and A. Berns.** 1990. Tumorigenesis by slow-transforming retroviruses-an update. Biochim. Biophys. Acta **1032:**213–235.
17. **Miller, A. D., and C. Buttimore.** 1986. Redesign of retrovirus packaging cell lines to avoid recombination leading to helper virus production. Mol. Cell. Biol. **6:**2895–2902.
18. **Miller, A. D., and G. J. Rosman.** 1989. Improved retroviral vectors for gene transfer and expression. BioTechniques **7:**980–990.
19. **Nagaya, T., T. Nakamura, T. Tokino, T. Tsurimoto, M. Imai, T. Mayumi, K. Kamino, K. Yamamura, and K. Matsubara.** 1987. The mode of hepatitis B virus DNA integration in chromosomes of human hepatocellular carcinoma. Genes Dev. **1:**773–782.
20. **Ogston, W., G. Jonak, C. Rogler, S. Astrin, and J. Summers.** 1982. Cloning and structural analysis of integrated woodchuck hepatitis virus sequences from hepatocellular carcinomas of woodchucks. Cell **29:**385–394.
21. **Popper, H., L. Roth, R. H. Prucell, B. C. Tennant, and J. L. Gerin.** 1987. Hepatocarcinogenicity of the woodchuck hepatitis virus. Proc. Natl. Acad. Sci. USA **84:**866–870.
22. **Rao, L., M. Debbas, P. Sabbatini, D. Hecenbery, D. Korsmeyer, and E.**

White. 1992. The adenovirus E1A proteins induced apoptosis, which is inhibited by the E1B 19kDa and bcl-2 proteins. Proc. Natl. Acad. Sci. USA **89:** 7742–7746.
23. **Reed, J. C.** 1994. Bcl-2 and the regulation of programmed cell death. J. Cell Biol. **124:**1–6.
24. **Robinson, W. S.** 1994. Molecular events in the pathogenesis of hepadnavirus-associated hepatocellular carcinoma. Annu. Rev. Med. **45:**297–323.
25. **Roe, T., T. C. Reynolds, G. Yu, and P. O. Brown.** 1993. Integration of murine leukemia virus DNA depends on mitosis. EMBO J. **12:**2099–2108.
26. **Sambrook, J., E. F. Fritsch, and T. Maniatis.** 1989. Molecular cloning: a laboratory manual, 2nd ed. Cold Spring Harbor Laboratory Press, Cold Spring Harbor, N.Y.
27. **Schirmacher, P., W. A. Held, D. Yang, F. V. Chisari, Y. Rustum, and C. E. Rogler.** 1992. Reactivation of insulin-like growth factor II during hepatocarcinogenesis in transgenic mice suggests a role in malignant growth. Cancer Res. **52:**2549–2556.
28. **Seeger, C., B. Baldwin, W. E. Hornbuckle, A. E. Yeager, B. C. Tennant, P. Cote, L. Ferrell, D. Ganem, and H. E. Varmus.** 1991. Woodchuck hepatitis virus is a more efficient oncogenic agent than ground squirrel hepatitis virus in a common host. J. Virol. **65:**1673–1679.
29. **Shih, C., K. Burke, M. J. Chou, J. B. Zeldis, C. S. Yang, C. S. Lee, K. J. Isselbacher, J. R. Wands, and H. M. Goodman.** 1987. Tight clustering of human hepatitis B virus integration sites in hepatomas near a triple-stranded region. J. Virol. **61:**3491–3498.
30. **Sladowski, D., S. J. Steer, R. H. Clothier, and M. Balls.** 1993. A improved MTT assay. J. Immunol. Methods **157:**203–207.
31. **Takagi, H., R. Sharp, C. Hammermeister, T. Goodrow, M. O. Bradley, N. Fausto, and G. Merlino.** 1992. Molecular and genetic analysis of liver oncogenesis in transforming growth factor α transgenic mice. Cancer Res. **52:** 5171–5177.
32. **Truant, R., J. Antunovic, J. Greenblatt, C. Prives, and J. A. Cromlish.** 1995. Direct interaction of the hepatitis B virus HBx protein with p53 leads to inhibition by HBx of p53 response element-directed transactivation. J. Virol. **69:**1851–1859.
32a. **Ueda, K., and Y. Wei.** Unpublished data.
33. **Varmus, H. E., T. Padget, S. Heasley, G. Simon, and J. M. Bishop.** 1977. Cellular functions are required for the synthesis and integration of avian sarcoma virus-specific DNA. Cell **11:**307–319.
34. **Wagner, A. J., M. Kokontis, and N. Hay.** 1994. Myc-mediated apoptosis requires wild-type p53 in a manner independent of cell cycle arrest and the ability of p53 to induce $p21^{waf1/cip1}$. Genes Dev. **8:**2817–2830.
35. **Wagner, A. J., M. B. Small, and N. Hay.** 1993. Myc-mediated apoptosis is blocked by ectopic expression of *bcl-2*. Mol. Cell. Biol. **13:**2432–2440.
36. **Wang, X., K. Forrester, H. Yeh, M. Feitelson, J.-R. Gu, and C. Harris.** 1994. Hepatitis B virus X protein inhibits p53 sequence-specific DNA binding, transcriptional activity and association with transcription factor ERCC 3. Proc. Natl. Acad. Sci. USA **91:**2230–2234.
37. **Wei, Y., G. Fourel, A. Ponzetto, M. Silvestro, P. Tiollais, and M.-A. Buendia.** 1992. Hepadnavirus integration: mechanisms of activation of the N-*myc2* retrotransposon in woodchuck liver tumors. J. Virol. **66:**5265–5276.
38. **White, E., R. Cipriani, P. Sabbatini, and A. Denton.** 1991. Adenovirus E1B 19-kilodalton protein overcomes the cytotoxity of E1A proteins. J. Virol. **65:** 2968–2978.
39. **White, E.** 1993. Death-defying acts: a meeting review on apoptosis. Genes Dev. **7:**2277–2284.
40. **Williams, G. T.** 1991. Programmed cell death: apoptosis and oncogenesis. Cell **65:**1097–1098.
41. **Williams, G. T., and C. A. Smith.** 1993. Molecular regulation of apoptosis: genetic controls on cell death. Cell **74:**777–779.
42. **Wu, X., G. Merlino, and N. Fausto.** 1994. Establishment and characterization of differentiated, nontransformed hepatocyte cell lines derived from mice transgenic for transforming growth factor α. Proc. Natl. Acad. Sci. USA **91:** 674–678.
43. **Yang, D., E. Alt, and C. E. Rogler.** 1993. Coordinate expression of N-myc2 and insulin-like growth factor II in precancerous altered hepatic foci in woodchuck hepatitis virus carriers. Cancer Res. **53:**2020–2027.
44. **Yang, D., and C. E. Rogler.** 1991. Analysis of insulin-like growth factor II (IGF II) expression in neoplastic nodules and hepatocellular carcinomas of woodchucks utilizing in situ hybridization and immunocytochemistry. Carcinogenesis **12:**1893–1901.
45. **Zoulim, F., J. Saputelli, and C. Seeger.** 1994. Woodchuck hepatitis X protein is required for viral infection in vivo. J. Virol. **68:**2026–2030.